Inorganic Chemistry

ARTICLE

pubs.acs.org/IC

On the High Magnetic-Ordering Temperature of the 5d Magnetic Oxide Ca_3LiOsO_6 Crystallizing in a Trigonal Crystal Structure: Density Functional Analysis

Erjun Kan,[†] Fang Wu,[‡] Changhoon Lee,[§] Jinhee Kang,[§] and Myung-Hwan Whangbo*[,§]

[†]Department of Applied Physics, Nanjing University of Science and Technology, Nanjing, Jiangsu 210094, People's Republic of China

[‡]School of Science, Nanjing Forestry University, Nanjing, Jiangsu 210037, People's Republic of China

[§]Department of Chemistry, North Carolina State University, Raleigh, North Carolina 27695, United States

ABSTRACT:

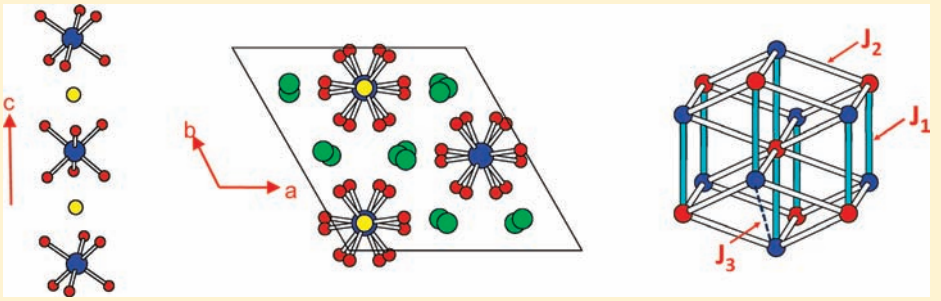

The 5d magnetic oxide Ca_3LiOsO_6 has a trigonal arrangement of its $LiOsO_6$ chains parallel to the c-direction and hence has triangular arrangements of high-spin Os^{5+} (d^3) ions but exhibits no spin frustration and undergoes a long-range antiferromagnetic ordering at a high temperature. The origin of this apparently puzzling observation was examined by evaluating the nearest-neighbor Os−O···O−Os spin exchange interactions of Ca_3LiOsO_6 on the basis of density functional calculations. Our study shows that, of the two nearest-neighbor interchain spin exchanges, one dominates over the other and that the intrachain spin exchange and the dominating interchain spin exchange are strong and form a three-dimensional antiferromagnetic spin lattice with no spin frustration, which is responsible for the long-range antiferromagnetic ordering of Ca_3LiOsO_6 at high temperature. In determining the strengths of the Os−O···O−Os exchange interactions of Ca_3LiOsO_6, the Li^+ and Ca^{2+} ions of the O···Li^+···O and O···Ca^{2+}···O linkages are found to play only a minor role.

1. INTRODUCTION

Recently, Yamaura and co-workers have synthesized the 5d magnetic oxide Ca_3LiOsO_6 containing high-spin Os^{5+} (d^3) ions and characterized its magnetic properties.[1] This compound, crystallizing in a trigonal space group $R3c$, has the K_4CdCl_6-type structure.[2] Namely, Ca_3LiOsO_6 consists of $LiOsO_6$ chains made up of the OsO_6 octahedra and LiO_6 trigonal prisms, which alternate by sharing their faces (Figure 1a). These $LiOsO_6$ chains, parallel to the c-direction and separated by Ca^{2+} ions, have a trigonal packing arrangement (Figure 1b).[1] The Os^{5+} (d^3) ions of Ca_3LiOsO_6 are well separated from each other, but the spin exchange interactions between their ions are strong because Ca_3LiOsO_6 undergoes a three-dimensional (3D) antiferromagnetic (AFM) ordering at a high temperature (i.e., 117 K).[1] This implies that the spin exchange interactions between the Os^{5+} ions, which occur through the Os−O···O−Os super-superexchange paths,[3] are strong. However, the trigonal arrangement of the $LiOsO_6$ chains (Figure 1b) raises an interesting question because it leads to triangular arrangements of the Os^{5+} ions (see Section 3). A triangular spin lattice with nearest-neighbor atomic force microscopy (AFM) spin exchange is spin frustrated[4] and is hence prevented from having a long-range magnetic ordering. For a magnetic system with spin frustration, it is generally expected that the ratio $f = |\theta|/T_N$, where θ and T_N are Curie−Weiss and Néel temperatures, respectively, is greater than 6.[4a] The f value for Ca_3LiOsO_6 is much lower than this critical value (i.e., $f \approx 2.2$, $\theta = -260$ K, $T_N = 117$ K). Similarly, high 3D AFM ordering temperatures were reported for the Ru-analogues of Ca_3LiOsO_6, namely, Sr_3NaRuO_6 ($T_N = 70$ K),[5] Sr_3LiRuO_6 ($T_N = 90$ K),[5] Ca_3NaRuO_6 ($T_N = 90$ K),[5,6] and Ca_3LiRuO_6 ($T_N = 120$ K).[5] The high T_N and low f values of Ca_3LiOsO_6 indicate that it has very weak spin frustration, if any. This in turn implies that triangles made up of AFM spin exchange paths are absent in the spin lattice of Ca_3LiOsO_6 although it has triangular arrangements of the Os^{5+} ions. This reasoning also applies to the isostructural/isoelectronic magnetic oxides Sr_3LiRuO_6, Sr_3NaRuO_6, Ca_3NaRuO_6, and Ca_3LiRuO_6. To verify the above implication, it is necessary to evaluate the spin exchanges

Received: February 14, 2011
Published: March 25, 2011

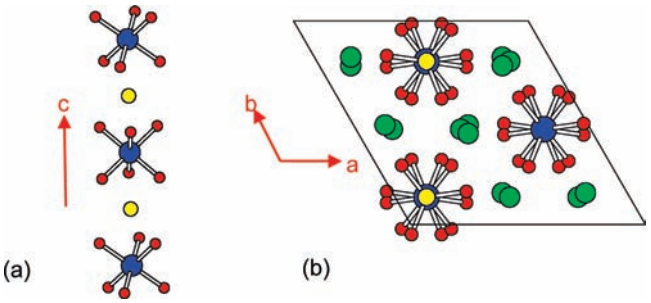

Figure 1. Structural features of Ca_3LiOsO_6: (a) A perspective view of an isolated $LiOsO_6$ chain made up of face-sharing OsO_6 octahedra and LiO_6 octahedra, where the blue, red, and yellow circles represent the Os, O, and Li atoms, respectively. (b) A projection view of Ca_3LiOsO_6 along the $LiOsO_6$ chain direction, where the green circles represent the Ca atoms.

of Ca_3LiOsO_6 and to identify its spin lattice on the basis of density functional calculations.

The oxygen atoms of the Os−O···O−Os exchange paths make contacts with the Li^+ or Ca^{2+} ions to form O···Li^+···O and O···Ca^{2+}···O linkages. In the case of Cs_2CuCl_4,[7] which is made up of $CuCl_4^{2-}$ molecular complexes separated by Cs^+ cations, the Cu−Cl···Cl−Cu spin exchanges are strongly affected by the 6p orbitals of the Cs^+ ions when two $CuCl_4^{2-}$ complexes plus the Cs^+ ions located between them have inversion or mirror-plane of symmetry. In addition, the interchain spin exchange interactions of cyano-bridged Ni^{2+}/M^{3+} (M = Cr, Fe, Co) chain complexes can be tuned by the size of the alkaline ion A^+ (A = Li, K, Rb, Cs).[8] Therefore, it is of interest to examine whether or not the Li^+ and Ca^{2+} cations play a significant role in making the Os−O···O−Os spin exchange interactions strong.

In the present work we explore the aforementioned questions about the magnetic properties of Ca_3LiOsO_6 on the basis of density functional calculations. We evaluate the strengths of intrachain and interchain Os−O···O−Os spin exchange interactions of Ca_3LiOsO_6 by performing mapping analysis based on density functional calculations.[3]

2. COMPUTATIONAL DETAILS

In our density functional calculations for Ca_3LiOsO_6, for which only the room-temperature crystal structure is known,[1] we employed the projector augmented wave (PAW) method encoded in the Vienna ab initio simulation package (VASP)[9] and the generalized gradient approximation (GGA) of Perdew, Burke, and Ernzerhof[10] for the exchange−correlation functional with the plane-wave cutoff energy of 500 eV and a set of 80 *k*-point for the irreducible Brillouin zone. To examine the effect of electron correlation in the Os 5d states, the GGA plus on-site repulsion method (GGA+U)[11] was used with the effective U_{eff} values of 0, 2.5, and 4.0 eV. To investigate how strongly the orbitals of the Li^+ and Ca^{2+} ions affect the Os−O···O−Os exchange interactions of Ca_3LiOsO_6, we studied the hypothetical systems $Ca_3A'OsO_6$ (A′ = Na, K) and A_3LiOsO_6 (A = Mg, Sr), respectively, in which the Li^+ and Ca^{2+} ions of Ca_3LiOsO_6 are replaced with other alkali and alkaline earth ions, respectively, without changing the crystal structure of Ca_3LiOsO_6.

3. SPIN EXCHANGE INTERACTION AND SPIN LATTICE

Figure 2 shows the total density of states (DOS) and the projected DOS (PDOS) for the Os 5d states, obtained for the ferromagnetic state of Ca_3LiOsO_6 by the GGA+U calculations

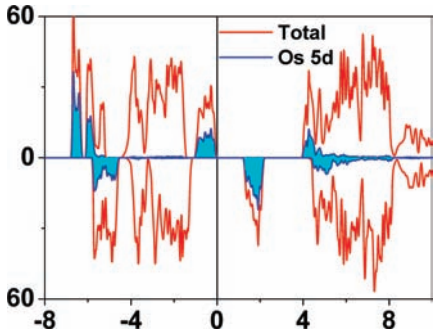

Figure 2. (a) Plots of the total DOS and the PDOS for the Os 5d states obtained for the ferromagnetic state of Ca_3LiOsO_6 from the GGA+U calculations with U_{eff} = 2.5 eV. The PDOS plot for the Os 5d states indicated by shading. The vertical axis represents the states/eV per six FUs, and the horizontal axis is the energy in eV. The up- and down-spin states are indicated by positive and negative DOS values, respectively.

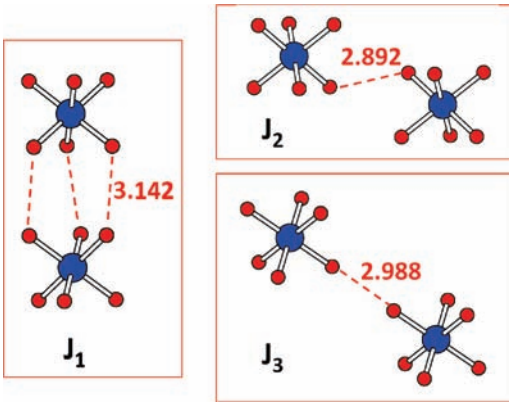

Figure 3. Pairs of OsO_6 octahedra associated with the intrchain spin exchange J_1 and the interchain spin exchanges J_2 and J_3, where the short O···O contact distances are given in Å.

with U_{eff} = 2.5 eV. The PDOS plot indicates that the filled up-spin t_{2g} bands are separated from the empty down-spin t_{2g} bands with a band gap, which is consistent with the experimental finding that Ca_3LiOsO_6 is a magnetic insulator with high-spin Os^{5+}. Though not shown, this finding is also true in the GGA+U calculations with U_{eff} = 0. These results agree with what Shi et al. reported from their density functional calculations.[1]

For the spin exchange interactions of Ca_3LiOsO_6, we consider the nearest-neighbor intrachain spin exchange J_1 as well as the nearest-neighbor interchain spin exchanges J_2 and J_3. The pairs of OsO_6 octahedra associated with these exchange paths are depicted in Figure 3, and the Os···Os and O···O distances associated with these paths are listed in Table 1. The magnetic orbitals of each Os^{5+} ion site are represented by the t_{2g} orbitals of its OsO_6 octahedron, in which the Os 5d orbitals are combined with the 2p orbitals of the surrounding O ligands (hereafter the O 2p tails) to make π^*-antibonding orbitals.[12] The spin exchange between two adjacent Os^{5+} ions are determined by the overlap between their t_{2g} orbitals, which is in turn determined by the overlap between their O 2p tails in the O···O contacts.[3]

How the exchange paths J_1−J_3 are arranged in a unit cell of Ca_3LiOsO_6 is depicted in Figure 4a, and an extended view of this arrangement is presented in Figure 4b. To evaluate the values of J_1−J_3, we first determine the relative energies of the four ordered

dx.doi.org/10.1021/ic200305a |*Inorg. Chem.* 2011, 50, 4182–4186

Table 1. Geometrical Parameters Associated with the Spin Exchange Paths J_1−J_3 in Ca_3LiOsO_6 and Values of J_1−J_3 in meV Obtained From GGA+U Calculations

	geometrical parameters		spin exchange		
	Os···Os (Å)	O···O (Å)	U_{eff} = 0 eV	U_{eff} = 2.5 eV	U_{eff} = 4 eV
J_1	5.390	3.142 (× 3)	−9.11	−4.42	−2.75
J_2	5.648	2.892 (× 1)	−3.97	−1.82	−1.09
J_3	6.448	2.988 (× 1)	−1.05	−0.28	−0.12

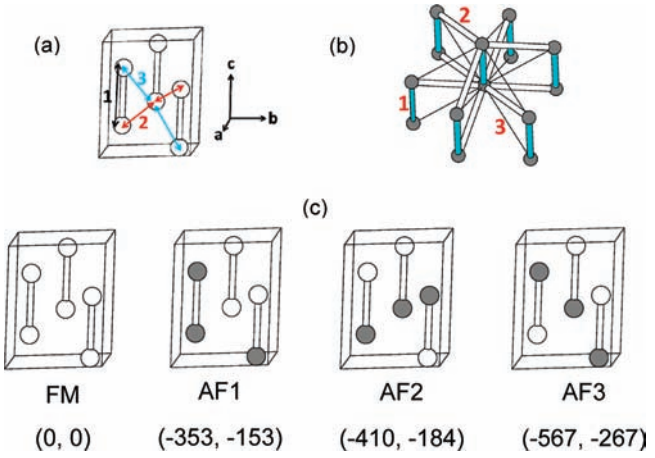

Figure 4. (a) Os−O···O−Os spin exchange paths J_1−J_3 in Ca_3LiOsO_6 defined by using one unit cell (containing six Os atoms), where only the Os atoms are shown for simplicity, and the numbers 1−3 refer to J_1−J_3, respectively. (b) Pattern of how the exchange paths J_1−J_3 occur in Ca_3LiOsO_6, where each $LiOsO_6$ chain is represented by two Os atoms (blue circles), and the numbers 1−3 refer to J_1−J_3, respectively. (c) Four ordered spin arrangements of Ca_3LiOsO_6 used to extract the J_1−J_3 values by mapping analysis, where the two numbers in each parentheses from left to right refer to the relative energies (in meV per six FUs), with respect to the ferromagnetic state, obtained from GGA+U calculations with U_{eff} = 0 and 2.5 eV, respectively.

spin states depicted in Figure 4c on the basis of GGA+U calculations with U_{eff} = 0 and 2.5 eV. The relative energies of these states obtained from our GGA+U calculations are summarized in Figure 4c. In terms of the spin Hamiltonian $\hat{H}=-\Sigma_{i<j}J_{ij}\hat{S}_i\cdot\hat{S}_j$, where J_{ij} = J_1 − J_3, the total spin exchange energies of these states per six formula units (FUs) are expressed as

$$\begin{aligned} E_{FM} &= (-6J_1 - 18J_2 - 18J_3)(N^2/4) \\ E_{AF1} &= (-2J_1 + 6J_2 + 6J_3)(N^2/4) \\ E_{AF2} &= (6J_1 - 6J_2 + 6J_3)(N^2/4) \\ E_{AF3} &= (6J_1 + 18J_2 - 18J_3)(N^2/4) \end{aligned} \quad (1)$$

by using the energy expressions obtained for spin dimers with N unpaired spins per spin site (in the present case, N = 3).[13] Thus, by mapping the relative energies of the four spin ordered states onto the corresponding energies expected from the total spin exchange energies, we obtain the values of J_1−J_3 summarized in Table 1.

To see how reasonable the calculated spin exchange parameters are, we calculate the Curie−Weiss temperature θ. In the mean field theory,[14] the θ for Ca_3LiOsO_6 is related to the spin

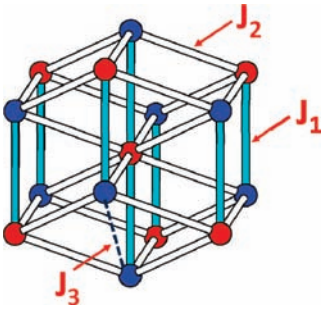

Figure 5. Three-dimensional antiferromagnetic spin lattice of Ca_3LiOsO_6 made up of the interchain exchanges J_1 (cyan cylinder) and J_2 (white cylinders), where the Os^{5+} (d^3) sites with different spins are distinguished by red and blue circles. The weak interchain exchanges J_3 (dashed line) occur between the blue circles in every quadrangle made up of four J_2 exchanges. Only one J_3 is shown for simplicity.

exchange parameters as follows:

$$\theta = \frac{S(S+1)}{3k_B}\sum_i z_i J_i \approx \frac{5(2J_1 + 6J_2 + 6J_3)}{4k_B} \quad (2)$$

where the summation runs over all nearest neighbors of a given spin site, z_i is the number of nearest-neighbors connected by the spin exchange parameter J_i, and S is the spin quantum number of each spin site (i.e., S = 3/2). Thus, the θ value is estimated to be −701, −311, and −185 K by using the spin exchange parameters from the GGA+U calculations with U_{eff} = 0, 2.5, and 4.0 eV, respectively. The experimental θ value of −260 K is reasonably well reproduced by the J_1−J_3 values obtained from the use of U_{eff} = 2.5 eV. Thus, hereafter, our discussion will be based on the results from the calculations with U_{eff} = 2.5 eV.

Our calculations show that the spin exchanges J_1−J_3 of Ca_3LiOsO_6 are all AFM, J_1 is the strongest spin exchange, $|J_2|/|J_1| \approx 0.4$, and $|J_3|/|J_1| \approx 0.06$. Thus, the spin exchange interactions of Ca_3LiOsO_6 are dominated by the intrachain exchange J_1 and the interchain exchange J_2, both of which are strong. As depicted in Figure 5, the exchanges J_1 and J_2 give rise to the 3D AFM spin lattice that contains only rings made up of four exchange paths: four J_2's, two J_1's plus two J_2's, and one J_1 plus three J_2's. Since this spin lattice does not contain any triangle made up of J_1 and J_2, there is no spin frustration in this 3D AFM spin lattice. The interchain exchange J_3 introduces weak spin frustration in every (J_1, J_2, J_3) triangle, but this effect should be negligible because J_3 is very weak compared with J_1 and J_2. (If J_3 were as strong as J_2, then the resulting spin lattice would be strongly spin frustrated, as can be seen from Figure 5.) Thus, the 3D AFM spin lattice made up of J_1 and J_2 explains why Ca_3LiOsO_6 undergoes a long-range AFM ordering at a high temperature (T_N = 117 K) despite its trigonal crystal structure[1] and also why Ca_3LiOsO_6 shows no major structural change at T_N.[1]

4. EFFECT OF LI^+ AND CA^{2+} IONS ON SPIN EXCHANGE

To examine the involvement of the orbitals of the Li^+ and Ca^{2+} cations in the spin exchange interactions of Ca_3LiOsO_6, we first inspect the PDOS plots calculated for the Li 2s/2p orbitals and for the Ca 4s/4p/3d orbitals (Figure 6). These plots indicate the presence of some Li^+ 2s/2p and Ca^{2+} 4s/4p/3d orbital contributions in the up-spin t_{2g} 5d block bands of Ca_3LiOsO_6. This indicates that the Li^+ and Ca^{2+} cations participate into the spin exchange interactions between the Os^{5+} ions. Incidentally,

dx.doi.org/10.1021/ic200305a |Inorg. Chem. 2011, 50, 4182–4186

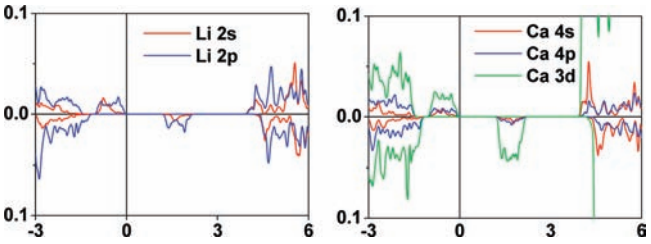

Figure 6. PDOS plots of (a) the Li 2s/2p and (b) the Ca 4s/4p/3d states obtained for the ferromagnetic state of Ca_3LiOsO_6 from the GGA+U calculations with U_{eff} = 2.5 eV. The vertical axis represents the states/eV per atom and the horizontal axis the energy in eV. The up- and down-spin states are indicated by positive and negative DOS values, respectively.

Table 2. Values of the Spin Exchange Parameters J_1−J_3 in meV of $Ca_3A'OsO_6$ and A_3LiOsO_6 Obtained from GGA+U Calculations with U_{eff} = 2.5 eV

$Ca_3A'OsO_6$	A′ = Li	A′ = Na	A′ = K
J_1	−4.42	−4.02	−3.14
J_2	−1.82	−1.90	−2.08
J_3	−0.28	−0.29	−0.32
A_3LiOsO_6	Mg	Ca	Sr
J_1	−2.47	−4.42	−5.04
J_2	−1.77	−1.82	−1.70
J_3	−0.15	−0.28	−0.27

it is interesting to note that, of the 4s, 4p and 3d orbitals of the Ca^{2+} ions, the 3d orbital contributes more strongly than do the 4s and 4p orbitals. A related observation to note is that the 3d orbitals of Ca are essential in producing the interlayer band of CaC_6[15] important for its superconductivity.

To further probe the participation of the Li^+ and Ca^{2+} cations in the spin exchanges of Ca_3LiOsO_6, we evaluate the spin exchange parameters J_1−J_3 for the hypothetical structures A_3LiOsO_6 (A = Mg, Sr) in which the alkaline earth ions A^{2+} occupy the Ca^{2+} sites of Ca_3LiOsO_6 as well as those for the $Ca_3A'OsO_6$ (A′ = Na, K) in which the alkali elements A'^{+} occupy the Li^+ sites of Ca_3LiOsO_6. Our results, summarized in Table 2, show that when the Li^+ ions are replaced with other alkali cations A'^{+}, the intrachain exchange J_1 becomes weaker with increasing the size of A'^{+} and the interchain exchanges J_2 and J_3 are more weakly affected. Likewise, when the Ca^{2+} cations of Ca_3LiOsO_6 are replaced with other alkaline earth cations A^{2+}, J_1 becomes stronger with increasing the A^{2+} cation size, and J_2 and J_3 are more weakly affected. Nevertheless, the trend in the relative strengths, $|J_1| > |J_2| \gg |J_3|$ found for Ca_3LiOsO_6, remains unchanged in $Ca_3A'OsO_6$ and A_3LiOsO_6. These observations indicate that, in determining the strengths of the Os−O···O−Os exchange interactions, the overlap between the two magnetic orbitals of the two Os^{5+} sites is governed largely by the overlap between their O 2p orbital tails[3] present on the O···O contact. The orbitals of the Li^+ and Ca^{2+} cations in the O···Li^+···O and O···Ca^{2+}···O linkages do not play a crucial role.

5. DISCUSSION

It should be emphasized that the 3D AFM spin lattice of Figure 5 is possible because, of the two nearest-neighbor interchain exchanges, one dominates over the other one (i.e., $|J_2| \gg |J_3|$). If both interchain exchanges were comparable in magnitude, then the spin lattice of Ca_3LiOsO_6 would be highly spin frustrated, as expected from its trigonal crystal structure. The high magnetic-ordering temperatures found for the Ru-analogues of Ca_3LiOsO_6, i.e., Sr_3LiRuO_6, Sr_3NaRuO_6, Ca_3NaRuO_6, and Ca_3LiRuO_6 can be similarly explained.

In the Os−O···O−Os spin exchange paths of Ca_3LiOsO_6, the O···O contact is shorter for the J_2 path than for the J_3 path (2.892 vs 2.988 Å, Figure 3), which makes J_2 stronger than J_3. Although the J_1 path has a longer O···O contact distance than does the J_2 path (3.142 vs 2.892 Å), J_1 is stronger than J_2. This is understandable because the J_1 path has three O···O contacts between the two OsO_6 octahedra so that the O 2p tails of their magnetic orbitals overlap significantly, whereas the J_2 path has only one short O···O contact. The O···O contact distance of J_1 will increase when Li^+ is replaced with Na^+, and J_2 will increase when Ca^{2+} is replaced with Sr^{2+}. The increase in the O···O contact distance will decrease the overlap between the O 2p tails involved. Thus, in the Ru-analogues of Ca_3LiOsO_6, the 3D AFM ordering temperature decreases in the order Ca_3LiRuO_6 (T_N = 120 K) > Sr_3LiRuO_6 (T_N = 90 K), Ca_3NaRuO_6 (T_N = 90 K) > Sr_3NaRuO_6 (T_N = 70 K).[5,6]

6. CONCLUDING REMARKS

The spin exchanges of Ca_3LiOsO_6 are dominated by the intrachain exchange J_1 and the interchain exchange J_2, which are strong and form a 3D AFM spin lattice with no spin frustration. The latter explains why Ca_3LiOsO_6 has a long-range AFM ordering at a high temperature (T_N = 117 K) although it consists of triangular arrangements of Os^{5+} ions. This AFM spin lattice with no spin frustration arises from the fact that, of the two nearest-neighbor interchain exchanges, one dominates over the other (i.e., $|J_2| \gg |J_3|$). The high magnetic-ordering temperatures of the Ru-analogues of Ca_3LiOsO_6, i.e., Sr_3LiRuO_6, Sr_3NaRuO_6, Ca_3NaRuO_6, and Ca_3LiRuO_6, can be similarly accounted for. In determining the strengths of the Os−O···O−Os exchange interactions of Ca_3LiOsO_6, the orbitals of the Li^+ and Ca^{2+} ions in the O···Li^+···O and O···Ca^{2+}···O linkages do not play an important role.

AUTHOR INFORMATION

Corresponding Author
*E-mail: mike_whangbo@ncsu.edu.

ACKNOWLEDGMENT

Work at NCSU by the Office of Basic Energy Sciences, Division of Materials Sciences, U.S. Department of Energy, under grant DE-FG02-86ER45259 and also by the computing resources of the NERSC center and the HPC center of NCSU.

REFERENCES

(1) Shi, Y.; Guo, Y.; Yu, S.; Arai, M.; Sato, A.; Belik, A.-A; Yamaura, K.; Takayama-Muromachi, E. *J. Am. Chem. Soc.* **2010**, *132*, 8474.
(2) Bergerhoff, G.; Schmitz-Dumont, O. *Z. Anorg. Allg. Chem.* **1956**, *284*, 10.
(3) Whangbo, M.-H.; Koo, H.-J.; Dai, D. *J. Solid State Chem.* **2003**, *176*, 417.
(4) (a) Greedan, J. E. *J. Mater. Chem.* **2001**, *11*, 37. and the references cited therein.(b) Dai, D.; Whangbo, M.-H. *J. Chem. Phys.* **2004**, *121*, 672.

(5) Darriet, J.; Grasset, F.; Battle, P. D. *Mater. Res. Bull.* **1997**, *32*, 139.
(6) Claridge, J. B.; Layland, R. C.; Adams, R. D.; zur Loye, H.-C. *Z. Anorg. Allg. Chem.* **1997**, *623*, 1131.
(7) Lee, C.; Kang, J.; Lee, K.; Whangbo, M.-H. *Inorg. Chem.* **2009**, *48*, 4165.
(8) Atanasov, M.; Comba, P.; Förster, S.; Linti, G.; Malcherek, T.; Miletich, R.; Prikhod'ko, A. I.; Wadepohl, H. *Inorg. Chem.* **2006**, *45*, 7722.
(9) (a) Kresse, G.; Hafner, J. *Phys. Rev. B* **1993**, *47*, 558. (b) Kresse, G.; Furthmüller, J. *Comput. Mater. Sci.* **1996**, *6*, 15. (c) Kresse, G.; Furthmüller, J. *Phys. Rev. B* **1996**, *54*, 11169.
(10) Perdew, J. P.; Burke, K.; Ernzerhof, M. *Phys. Rev. Lett.* **1996**, *77*, 3865.
(11) Dudarev, S. L.; Botton, G. A.; Savrasov, S. Y.; Humphreys, C. J.; Sutton, A. P. *Phys. Rev. B* **1998**, *57*, 1505.
(12) Albright, T. A.; Burdett, J. K.; Whangbo, M.-H. *Obital Interactions in Chemistry*; Wiley: New York, 1985.
(13) (a) Dai, D.; Whangbo, M.-H. *J. Chem. Phys.* **2001**, *114*, 2887. (b) Dai, D.; Whangbo, M.-H. *J. Chem. Phys.* **2003**, *118*, 29.
(14) Smart, J. S. *Effective Field Theory of Magnetism*; Saunders: Philadelphia, PA, 1966.
(15) Deng, S.; Simon, A.; Köhler, J. *Angew. Chem., Int. Ed.* **2008**, *47*, 6703.